電子束石版術中蒙地卡羅模擬程式之發展

計畫編號：NSC89-2215-E009-096
執行期限：89/08/01～90 /07/31
主持人：郭雙發 國立交通大學電子研究所教授
E-mail：sfguo@cc.nctu.edu.tw
計畫參與人員：黃琪聰、蔡銘仁 國立交通大學電子研究所

一、中文摘要

吾人利用蒙地卡羅方法發展出電子束石版術之模擬程式，其中電子和核子間的彈性碰撞係用拉塞福公式決定，而其能量損失則用貝茲公式計算。我們可獲得在光阻及基材中電子軌跡的三維空間分佈、能量沉積的分佈，藉以了解電子束石版術的漸近效應。為了獲得適當的精確度，曝照欄框的蒙地卡羅模擬通常需採樣大量的入射點和電子數，因而耗費冗長的計算時間。為了避免此一缺失，本程式乃採取電子雲策略及迴旋積分方法來縮短模擬時間。

關鍵詞: 蒙地卡羅模擬、電子束石版術、彈性碰撞、電子雲、迴旋積分方法

Abstract:

A Monte Carlo simulation program for the electron-beam lithography has been developed. The screened Rutherford equation for the differential scattering cross section and the Bethe equation for the energy loss between elastic scatterings are used. Three dimensional electron trajectories in the resist and substrate have been followed. The lateral spreading range and longitudinal penetration depth of energy deposition have been obtained. An “electron cloud” scheme has been adopted in this program to reduce the simulated particles and computational time. A convolution method has been devised to extend the simulated energy deposition distribution.

Keyworks: Monte Carlo simulation, E-Beam lithography, elastic scattering, electron cloud, convolution method.

二、緣由與目的

電子工業已是台灣最主要的高科技產業，其中又以半導體工業為主。半導體工業發展的最重要驅動力量在於石版術的驚人進步，它將積體電路設計規則的尺度以指數的速率縮小：由 1970 年的 10 微米(μm)降至 2000 年的 180 奈米(nm)。電子束石版術為超大規模集積(VLSI)電路光罩製作的主要方法，石版術的重要性可由半導體工廠中光罩及相關的照相蝕刻等設備之投資往往佔產品百分之四十的成本看出。

在半導體元件的大量生產方面，光學石版術一直都擔任重要的角色，亦確屬微電子工業的生機根源。然而，這些元件的設計規則在進入 180 奈米的門檻以後，光學石版術的解析能力卻面臨到光學繞射的物理極限，即使是採用 KrF 激二體(excimer)雷射(248 奈米)石版術及光學石版術解析度增強技術(RET)亦有其圖案安排上的限制。因此，電子束石版術很有希望取代光學石版術的地位，由於它具有較高的解析度、較深的焦距深度和無光罩的操作等潛能。

電子束石版術的終極解析度並非由電子光學系統之解析度所限，它能夠趨近於 0.1 奈米，而是由阻劑的解析度和隨後的製作程序所限，其重要的限制是阻劑中的電子散射。順向散射是電子在貫穿阻劑時的小角度非彈性散射，它具有較窄的分佈。背向散射是大角度彈性散射，主要發生在阻劑底下的基片，電子從基片背向散射進入阻劑中，產生一種背景模糊的影像，降低了明確的對比，而其終極影響是臨近效應。在電子束石版術中，圖案裡任何一點的曝照都會被緊臨該點的欄框之曝照所影響。為了減小其效應，亟需發展精巧的計算方法以資調整各種形狀的曝照劑量，其中應以蒙地卡羅模擬計算為最佳選擇。

電子束多層多元素標靶中的滲透和散射，實際上唯有求助於蒙地卡羅方法才能精確地計算出電子束的曝照分佈以及背向散射電子的能量和角向分佈。這種方法的優點是可以將各種物理程序直接包括在內，並處理各種複雜的幾何形狀。其缺點則為需要耗費大量的計算時間，因為各種分佈的任何參數之相對誤差約略地比例於入射電子數目的平方根之倒數。然而，現今計算機的運算速度日益增快，入射電子數目已可大量的增加，以獲得任意的精確度。

電子束石版術的蒙地卡羅模擬研究雖然在國外已有二十多年的歷史，但是在國內還沒有人從事這方面的研究，只有本計劃主持人做過類似的離子植入蒙地卡羅模擬。本專題研究就是沿用以往的經驗，將離子改為電子並代換以適當的碰撞機制。

三、物理模式

Elastic scattering between incident electron and nucleus of target atom is based on Rutherford equation for the differential scattering cross section [1]:

$$\frac{d\pm}{d\Omega} = \left(\frac{Ze^2}{8\pi\varepsilon_0 E}\right)^2 \left(\frac{1}{1-\cos\theta + 2\alpha}\right)^2 \qquad (1)$$

where θ is the scattering angle, Z is the atomic number of the target atoms, e is the electric charge of an

electron, ε_0 is the permittivity of free space, E is the electron energy and α represents an effective screening parameter of the electronic cloud on the nuclear charge. The parameter α is given by [2]:

$$\alpha = 0.25\left(\frac{1.12\hbar Z^{\frac{1}{3}}}{0.885 a_0 p}\right)^2 \qquad (2)$$

where $\hbar$ is the reduced Planck constant, a_0 is the Bohr radius of the hydrogen atom, p is the momentum of the incident electron.

The total elastic cross section σ can be obtained by integrating equation (1) as

$$\sigma = \left(\frac{Ze^2}{8\pi\varepsilon_0 E}\right)^2 \left(\frac{\pi}{\alpha(\alpha+1)}\right) \quad \text{m}^2 \qquad (3)$$

The energy loss model of our simulator is basically the Bethe equation [3]:

$$\frac{dE}{ds} = -2\pi\left(\frac{e^2}{4\pi\varepsilon_0}\right)^2 \frac{NZ}{E}\ln\left(\frac{\gamma E}{J}\right) \quad \text{joule/m} \qquad (4)$$

where N is the number density, $\gamma = 1.1658$ and J represents the mean excitation energy in the solid.

$$J = (9.67Z + 58.8Z^{-0.19}) \quad \text{eV} \qquad (5)$$

In order to avoid the failure of Bethe equation (4) at low energy $(E \le J/1.116)$ we use the parabolic extrapolation of $(dE/ds)^{-1}$ proposed by Rao-Sahib and Witty [4] for $E < 6.338J$.

$$\frac{dE}{ds} = -2\pi\left(\frac{e^2}{4\pi\varepsilon_0}\right)^2 \frac{NZ}{1.26\sqrt{JE}} \qquad (7)$$

In this way the trajectory of each electron can be pursuit down to 50eV instead of the commonly used cut-off energy 500eV.

In case of compound materials, the weight individual contributions of the atoms have to be used [5]:
For high electron energy,

$$\frac{dE}{ds} = -\frac{2\pi}{E}\left(\frac{e^2}{4\pi\varepsilon_0}\right)^2 \sum_i \left[N_i Z_i \ln\left(\frac{\gamma E}{J_i}\right)\right] \qquad (8)$$

For low electron energy,

$$\frac{dE}{ds} = -2\pi\left(\frac{e^2}{4\pi\varepsilon_0}\right)^2 \frac{1}{1.26}\sum_i \left(\frac{N_i Z_i}{\sqrt{J_i E}}\right) \qquad (9)$$

where N_i is the number of atoms of the i^{th} species

$$N_i = \rho N_A \frac{m_i}{\sum_j m_j A_j} \qquad (10)$$

and $\sum_j m_j A_j$ sums up to be the molecular weight.

四、蒙地卡羅方法

Both elastic and inelastic scattering events occur according to given probabilities and statistical information is extracted about microscopic variables of interest. Due to the statistical nature of the simulated process, a quite large number of electron trajectories are required in order to obtain sufficient accuracy in the results.

A random number R_1, uniformly distributed between 0 and 1, is first invoked for deciding the free path length Δs traveled between two subsequent collisions [6], [7].

$$\Delta s = -\lambda \ln(R_1) \qquad (11)$$

the mean free path is

$$\lambda = \frac{1}{\sum_i N_i \sigma_i} \qquad (12)$$

where σ_i is the total elastic cross section relative to the atom of the i^{th} species.

A second random number R_2 determines the atom species involved in the collision. Taking into account that the probability P_i of scattering from an atom of the i^{th} species is proportional to $N_i\sigma_i$ and $\sum_i P_i = 1$, we have

$$P_i = \frac{N_i\sigma_i}{\sum_i N_i\sigma_{ii}} \qquad (13)$$

Thus, the interval [0, 1] is divided in segments of length P_i. The type of atom acting as scattering center is given by the value of R_2.

The azimuthal angle is ranging between 0 and 2π in equal probability and is given by the random number R_3,

$$\phi = 2\pi R_3 \qquad (14)$$

The probability of scattering angle, which range is equal probability between 0 and π

$$\cos\theta = 1 - \frac{2\alpha R_4}{1+\alpha-R_4} \qquad (15)$$

where R_4 is also [0,1]

五、結果與討論

Figure 1 shows the scattering trajectories of 100 simulated electrons with incident energies of 20keV in a target of PMMA (0.5 μm) / SiO_2 (0.5 μm) / Si (5 μm). Some electrons travel a long distance with a small energy loss. The back scattering electrons from Si substrate into resist will expose the resist, which we don't want to. This effect is call proximity effect.

Figure 2 plots the electron scattering range as a

function of target density for two different incident energies. Note that the data points in Figure 2 are the simulated results for PMMA (ρ =0.94 g/cm^3), Si (ρ =2.328 g/cm^3), GaAs (ρ =5.32 g/cm^3), and Au (ρ =19.3 g/cm^3), while the solid and dashed curves are empirically fitted to the following relation.

$$Range(E_i, \rho) = 11.52 E_i^{1.694} \rho^{-0.92} \qquad (16)$$

This equation is good enough to predict the range of electrons incident to different target materials with different incident energies. The electron ranges are almost inversely proportional to the target density.

Figure 3 shows the energy distribution along depth z. Peak energy intensity is near the interface of resist and substrate. Most of electrons are collision near the interface of resist and substrate, so they have greater probability to go back to resist.

Figure 4 shows the effect of incident electron energy on the width and intensity of energy deposition density. As the energy of incident beam increases, the backscattered exposure spreads more and more. According to above reason this is very difficult to trade off the resolution and proximity. Higher energy is good for resolution, but is bad for proximity effect.

For energy deposition in lateral spreading, the range is defined as the standard deviation. Figure 5 shows the energy deposition range as a function of incident energy. The backward scattering energy range in the resist is almost proportion to incident energy. Electrons penetrate the resist layer of 500nm and enter into Si substrate when their energies are over 5keV. The forward scattering energy range is saturated at the value corresponding to the incident energy of 5keV.

Qualitatively, skewness measures the asymmetry of the distribution and kurtosis measures how flat the top of a distribution. Figure 6 shows the skewness and kurtosis for energy deposition distribution along y-axis in resist by backward scattering. It is well known that Gaussian distributions have a skewness of 0 and a kurtosis of 3. From the results of Figure 6 we can assume that the energy deposition density distributions within the resist by backward scattering behave as Gaussian distributions.

In discrete from, the convolution integer may be written as a convolution sum

$$g[n] = \sum_{k=-\infty}^{\infty} f[k]h[n-k] \qquad (17)$$

where $f[n]$ is the arbitrary input, $h[n]$ is the impulse response and $g[n]$ is called the convolution sum. In two-dimension, the convolution integral and convolution sum, (17) can be extended as

$$g[n,m] = \sum_{l=-\infty}^{\infty} \sum_{k=-\infty}^{\infty} f[k,l]h[n-k,m-l] \qquad (18)$$

Figure 7 shows the results of 2D energy deposition along lateral direction y within the photo resist for pattern width of 1000nm using convolution method.

六、結論

The Monte Carlo simulation programs developed in this work are very useful to the electron-beam lithography. We can follow the electron trajectories in resist and substrate. An empirical result of the spreading range as a function incident energy and target material density is very important to process design. The lateral spreading of energy deposition is the main limitation of electron-beam lithography. Spreading range is small for lower incident energy, but electrons may not penetrate resist at this energy. The convolution integral is very powerful to extend the energy distribution.

七、參考文獻

[1] G. Baccarain, "Process and Modeling for Microelectronics", Elsevier Science Publishers B.V. , 1993.

[2] B. P. Nigam, M. K. Saunderson and Ta-You Wu, Phys. Rev., 115(1959) 491.

[3] H. A. Bethe, Ann. Phys. (Leipz.), 5(1930) 325; Handb. Phys., 24(1933) 273.

[4] T. S. Rao-Sahib and D. B. Wittry, J. Appl. Phys., 45(1974) 5060.

[5] D. F. Kyser and K. Murata, "Quantitative Electron Microprobe Analysis of Thin Film on Substrates", IBM J. RES. DEVELOP. 1973, 352-362.

[6] J. Georgiev, G. Mladenov, D. Ivanov, "Monte Carlo simulation of electron-beam exposure distributions in the resist on structures with high -T_c superconducting thin films", Thin Solid Films, 251(1994) 67-71.

[7] Y. M. Gueorguiev, "A Program for Monte Carlo simulation of penetration and scattering of accelerated electrons in multicomponent multiplayer targets", Vacuum, volume 47, number 10, 1996, 1227-1230.

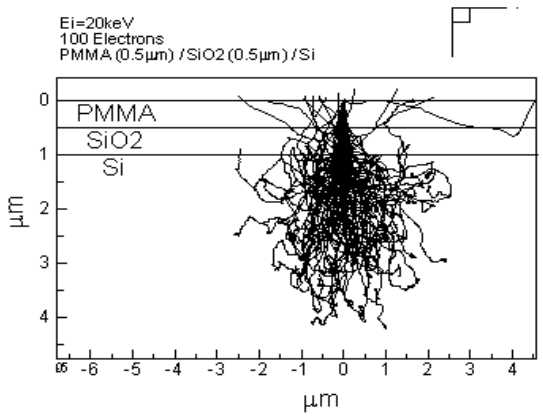

Figure 1. Electron scattering trajectories with incident energy 20keV in a target of PMMA (0.5 μm) / SiO_2 (0.5 μm) / Si (5 μm).

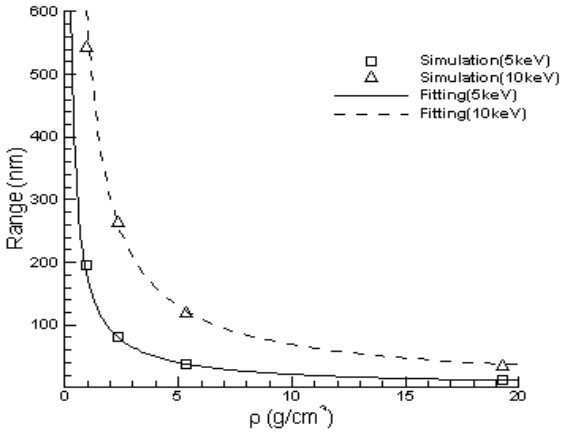

Figure 2. Range as a function of target density for two different incident energies

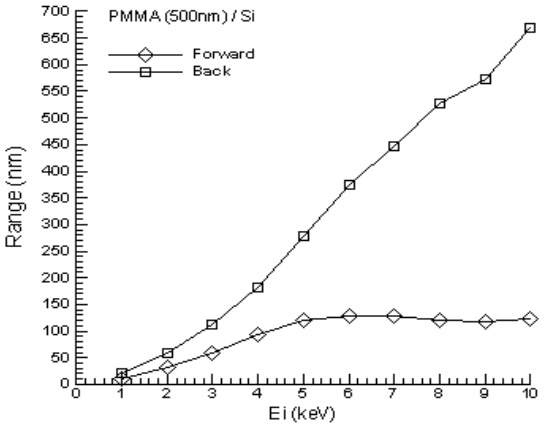

Figure 5. Energy deposition range as a function of incident energy in the resist

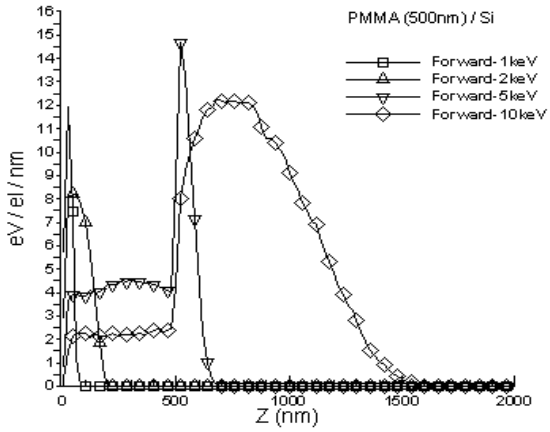

Figure 3. The forward scattering energy deposition at depth Z for resist thickness 500nm coating on Si substrate.

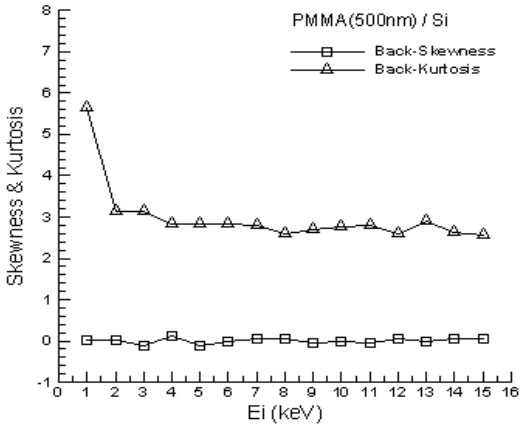

Figure 6. The skewness and kurtosis of energy distribution in the resist along y-axis by backward scattering

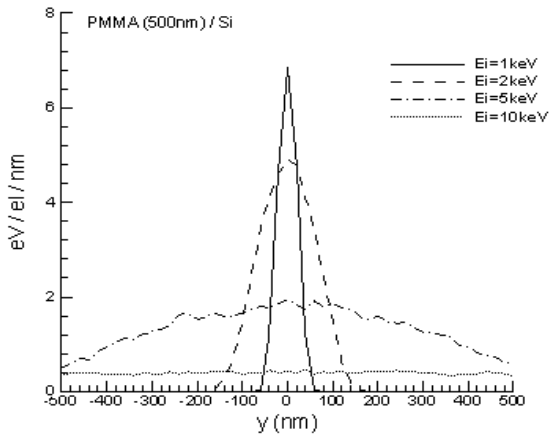

Figure 4. Energy deposition density for back scattering

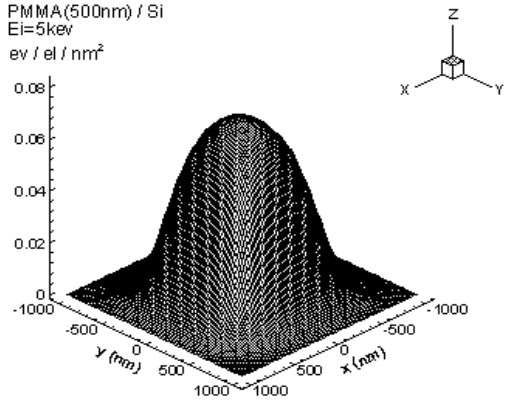

Figure 7. 2D Energy deposition profile used convolution method for pattern width1000nm.